

Modeling the therapeutic potential of defective interfering particles in the presence of immunity

Bandita Karki,¹ James J Bull,² and Stephen M Krone^{1,*†}

¹Department of Mathematics and Statistical Science, University of Idaho, Moscow, ID 83844-1103 USA and ²Department of Biological Sciences, University of Idaho, Moscow, ID 83844-3051 USA

[†]<https://orcid.org/0000-0002-9561-6996>

*Corresponding author: E-mail: krone@uidaho.edu

Abstract

Defective interfering particles (DIPs) are naturally occurring viruses that have evolved to parasitize other viruses. They suppress wild-type (WT) virus infections through their role as intracellular parasites. Because most encode few or no viral proteins, they have been entertained as possible safe antiviral therapies—something that might be given to patients infected with the WT virus. Adding to their safety, they cannot reproduce except when co-infecting the same cells as the WT, so they pose no danger of evolving into independent disease agents. But this dependence on the WT also limits their therapeutic utility by restricting the timing at which their administration can be effective. To develop a qualitative sense of these constraints for acute viral infections, we use ordinary differential equation models to study the mass-action dynamics of DIPs and WT virus in the presence of adaptive and innate immunity that will otherwise clear the infection. Our goal is to understand whether the therapeutic administration of DIPs will augment or interfere with the immune response and, in the former case, we seek to provide guidance on how virus suppression is affected by infection and clearance parameters, as well as by the timing of DIP introduction. Consistent with previous theoretical work, we find that DIPs can significantly suppress viral load. When immunity is present, the timing of DIP administration matters, with an intermediate optimum. When successful at viral suppression, DIPs even slow the immune response, but the combined effect of DIPs and immunity is still beneficial. Outcomes depend somewhat on whether immunity is elicited by and clears DIPs, but timing appears to have the greater effect.

Introduction

Defective interfering particles (DIPs) are viruses that have evolved to parasitize other viruses and are thought to arise naturally through spontaneous deletions. They are known from many RNA viruses (Dimmock and Easton, 2014; Vignuzzi and López, 2019; Alnaji and Brooke, 2020) and some DNA viruses (Horiuchi, 1983). They cannot reproduce on their own, requiring co-infection with the wild type (WT) into the same cell to produce progeny. They then vastly out-reproduce the WT by virtue of genomic modifications that enable them to usurp the WT proteins (small genome size, little or no gene expression, and extra regulatory signals). DIPs are subject to the usual density-dependent dynamics of all parasites, but the problem is more complicated because it involves three layers: cells, viruses as parasites of those cells, and DIPs as parasites of viral infections. One basic biological property of DIPs is that they do not persist at low densities of the WT virus.

As therapeutic agents, DIPs have two downsides that are relevant for therapy. First most DIPs are specific to a single WT virus, often to just individual strains of the WT (Barrett and Dimmock, 1986), although broader specificity has been noted with some

DIPs of influenza A virus (Dimmock et al., 2008; Dimmock and Easton, 2014). WT viruses and their natural DIP variants typically have co-evolved in an antagonistic arms race that leads to high specificity (Horiuchi, 1983; DePolo, Giachetti and Holland, 1987). Thus, DIP therapy potentially needs to be developed for each viral type unless non-specific, broad-range DIPs can be identified. Second, for most acute viral infections, rapid viral clearance or host death is the expected outcome in a short time frame. DIP use in acute infections must, therefore, be administered early enough to be effective but not so early that DIPs have decayed before infection.

DIPs could be studied at two different biological scales: within-cell processes and between-cell processes. Our focus here is on the latter, specifically with respect to (1) timing and (2) the suppressive effect of DIPs on viral densities. Furthermore, (3) we embed these processes in the host immune response. We apply simple models in the hope of capturing qualitative properties of DIP and viral dynamics. Simplicity is further justified because there are few empirical viral–DIP systems studied sufficiently to allow the direct model parameterization, although a few papers (e.g. Akpinar, Inankur and Yin (2016)) fit models to dynamic observations *in vitro*.

Our study in context

Previous mathematical models of temporal DIP dynamics (Bangham and Kirkwood, 1990; Kirkwood and Bangham, 1994; Frank, 2000; Akpinar, Inankur and Yin, 2016) have discovered basic properties of DIP–WT interactions: (1) DIPs cannot be maintained unless the WT is at sufficiently high density; (2) in mass action models, DIPs and WT exhibit damped oscillations or, if spontaneous WT and DIP mutations are allowed, sustained oscillations; (3) with spatial structure, the speed and structure of virus–DIP plaque formation are strongly governed by the ratio of DIPs to WT virus in the single inoculating (co-infected) cell.

Our work builds on this prior work but goes beyond by addressing DIPs in a therapeutic context, specifically a context in which the infection is eventually cleared by an immune response. This property fundamentally changes the behavior that can be studied because the viral endpoint is now extinction; the emphasis must be shifted to short-term dynamics and interaction with immunity. We provide ordinary differential equation (ODE) models that are intended to capture features of the time course of a continuous *in vivo* infection. For simplicity, we ignore the spatial structure, which has been shown to produce interesting spatiotemporal dynamics in partial differential equation (PDE) (Frank, 2000) and cellular automata (CA) (Akpinar, Inankur and Yin, 2016) models, but we do include the effects of innate and adaptive immunity, which we consider to be the main contribution of our paper. The time frame we imagine covers a period of a few weeks, especially in the presence of an immune response that can clear the virus. Other models (Bangham and Kirkwood, 1990; Kirkwood and Bangham, 1994; Frank, 2000) are more relevant for *in vitro* dynamics over a longer time, possibly involving repeated passaging that pulses the dynamics with periodic dilutions of WT virus and DIPs, along with supplementation of uninfected cells. For these long-term *in vitro* studies, it is natural to include mutations in both WT and DIP populations. Passaging and inclusion of mutations can contribute to more sustained oscillations in WT and DIP concentrations. In our short-term continuous models, mutation can be ignored as a first approximation and we observe damped oscillations that are consistent with ODE models in Frank (2000) when dead cells are replaced at a high rate; our models immediately replace dead infected cells with uninfected cells, thus maintaining a constant cell population size. Some other models in the literature (Thompson, Rempala and Yin, 2009; Thompson and Yin, 2010) focus on simple input–output relations or related difference equations for a few passages and are mostly meant to complement empirical results and estimate parameters.

We see our models as providing big-picture guidance for empirical work, as well as providing a starting point for more detailed models. Our goal is to attract an audience of empiricists, as well as some mathematical modelers, by using relatively simple mass-action differential equation models. We seek to gain some insight into DIP + WT dynamics and then, most importantly, to see how these dynamics interact with immune dynamics. One specific goal is to understand whether the therapeutic use of DIPs will enhance or interfere with immune system dynamics, and whether the timing of DIP therapy will influence the outcome. Our assumptions are guided by empirical data. For example, Dimmock and Easton (2014) reported data that put the progeny of DIP + WT co-infected cells at >99 per cent DIPs. This percentage no doubt depends on the particular WT/DIP pairing, but it at least closely approaches our assumption of 100 per cent DIP progeny. Thus we chose to exclude a tiny amount of WT

“leaking” from doubly infected cells, in agreement with other models (Kirkwood and Bangham, 1994; Frank, 2000); this omission probably has very little effect on dynamics. Getting the exact tiny fraction right for a particular example or running through a broad spectrum of possibilities is not the goal here, so we chose a simplification that very closely matches empirical data and allows us to more clearly delineate certain effects without muddying the waters with nuances of detail. Similarly, we ignored stochastic effects and time delays because our interest was in broad patterns.

Another simplification we employ involves immune system dynamics. One is invariably faced with the choice of specifying many details for which no parameterization is possible (e.g. the many immune cell types, the interactions between cells and secreted molecular signals such as interferons, and the spatial structure) versus merely specifying innate and adaptive immunity as two quantities that respond to pathogen density. Pragmatism dictates the latter path, which is what we applied.

Foundation: models lacking immunity

We begin by introducing a model (and a reduced version of that model) that characterizes interactions between WT virus, DIPs, and uninfected cells, but without any immune dynamics. These components will be retained in our model with immunity. Studying them separately, at first, will provide a baseline of WT suppression to be expected from DIPs alone. This will allow us to more accurately portray the effects of DIPs in the presence of immunity. Moreover, we will see that our simple characterization of DIP–WT dynamics, which ignores free virus and other complexities, manages to capture some of the key behaviors observed in other models. These behaviors include damped oscillations via predator–prey-like dynamics that accelerate DIP-based suppression of WT when WT densities are large.

Two simple ODE models are presented in this section: a ‘full’ model (Model 1) and a ‘reduced’ model (Model 2). Both ignore immunity but capture the basic dynamics between DIPs, WT virus, and cells. Both models describe fractions of cells that are infected with WT virus (V), co-infected with both DIPs and WT virus (B), and uninfected (E). The two models differ in whether they include (Model 1) or omit (Model 2) a term for cells infected with DIPs alone (D). By assumption $V + B + D + E = 1$, whether D is included or not. The full model includes $D > 0$, but Model 2 is included because it simplifies analytical solutions. Model variables and parameters are summarized in Table 1.

Model 1: Full DIP model

$$\begin{aligned}\dot{V} &= \beta_V V E - \beta_D B V - \delta_V V \\ \dot{B} &= \beta_D B V + \beta_V V D - \delta_B B \\ \dot{D} &= \beta_D B E - \beta_V V D - \delta_D D \\ \dot{E} &= -\dot{V} - \dot{B} - \dot{D}\end{aligned}\quad (1)$$

Model 2: Reduced DIP model

$$\begin{aligned}\dot{V} &= \beta_V V E - \beta_D B V - \delta_V V \\ \dot{B} &= \beta_D B V - \delta_B B \\ \dot{E} &= -\dot{V} - \dot{B}\end{aligned}\quad (2)$$

Table 1. Description of state variables and parameters common to all mathematical models ($D=0$ and $\delta_D=\infty$ are implicit in Model 2).

Notation	Description	Values
V	Fraction of cells infected by WT virus	[0,1]
B	Fraction of cells co-infected by WT virus and DIPs	[0,1]
D	Fraction of cells infected by DIPs	[0,1]
E	Fraction of uninfected cells	[0,1]
β_V	Infection rate by WT virus	2, 3
β_D	Infection rate by DIPs	1-5
δ_V	Death rate of cells infected with WT virus	1
δ_B	Death rate of cells co-infected with WT virus and DIPs	1
δ_D	Death rate of cells infected with DIPs	0.75-3

Each mass-action term in the two models lists the ‘donor’ first and the ‘recipient’ second. For example, the VD term in Model 1 corresponds to the virus from a V -infected cell infecting a D -infected cell, turning the D -infected cell into a B -infected cell while not changing the V donor. These asymmetries allow maintaining constant cell densities and match viral/DIP biology, such as the fact that a DIP-infected cell cannot infect other types of cells. Unlike previous models, we simplify the system by not tracking free virus. For example, the viral progeny from a V -infected cell are assumed to settle on cells of different types according to their frequencies, and some viral progeny might degrade before infecting a cell. Thus, the β terms combine burst size (or budding rate) and attachment and decay rates. We assume that co-infected cells produce only D progeny, in approximate agreement with empirical results (Dimmock and Easton, 2014) and providing a best case for DIP suppression of virus. Model 2 is the simplest and can be obtained by letting $\delta_D \rightarrow \infty$ in Model 1.

These differential equations follow the compartmental ‘SIS model’ approach from epidemiology, tracking frequencies (or densities) of susceptible and infected hosts (in this case with two possible infecting strains) and ignoring the dynamics of free virus and free DIPs. There is added complexity over typical two-strain SIS (susceptible-infective-susceptible) models, however, in that the WT virus is a parasite of cells and the DIPs are parasites of WT viruses (and cells).

Analytical properties of Models 1 and 2

Using ‘hat’ and ‘tilde’ to indicate equilibrium values that come from Model 1 and Model 2, it is easy to see that the two boundary equilibria are the same for both models:

- virus but no DIPs: $(\widehat{V}_1, \widehat{B}_1, \widehat{D}_1, \widehat{E}_1) = (1 - \frac{\delta_V}{\beta_V}, 0, 0, \frac{\delta_V}{\beta_V})$, $(\widetilde{V}_1, \widetilde{B}_1, \widetilde{E}_1) = (1 - \frac{\delta_V}{\beta_V}, 0, \frac{\delta_V}{\beta_V})$, and
- no virus and no DIPs: $(\widehat{V}_2, \widehat{B}_2, \widehat{D}_2, \widehat{E}_2) = (0, 0, 0, 1)$, $(\widetilde{V}_2, \widetilde{B}_2, \widetilde{E}_2) = (0, 0, 1)$.

It is also easy to confirm that the interior (coexistence) equilibrium $(\widetilde{V}_3, \widetilde{B}_3, \widetilde{E}_3)$ for Model 2 is given by

$$\widetilde{V}_3 = \frac{\delta_B}{\beta_D}, \quad (3)$$

$$\widetilde{B}_3 = \frac{\beta_V}{\beta_V + \beta_D} \left(1 - \frac{\delta_V}{\beta_V} - \frac{\delta_B}{\beta_D} \right), \quad (4)$$

$$\widetilde{E}_3 = 1 - \frac{\delta_B}{\beta_D} - \frac{\beta_V}{\beta_V + \beta_D} \left(1 - \frac{\delta_V}{\beta_V} - \frac{\delta_B}{\beta_D} \right). \quad (5)$$

This interior equilibrium exists when $1 - \frac{\delta_V}{\beta_V} - \frac{\delta_B}{\beta_D} > 0$. Thus, in the case of coexistence of DIPs and WT virus in Model 2, we see that (at equilibrium) DIPs suppress WT virus by an amount $\widetilde{V}_1 - \widetilde{V}_3 = 1 - \frac{\delta_V}{\beta_V} - \frac{\delta_B}{\beta_D}$, precisely the quantity that must be positive to guarantee long-term persistence of DIPs. The Jacobian at the interior equilibrium for Model 2 is

$$J = \begin{bmatrix} -\beta_V \frac{\delta_B}{\beta_D} & -(\beta_V + \beta_D) \frac{\delta_B}{\beta_D} \\ \frac{\beta_V \beta_D}{\beta_V + \beta_D} (1 - \frac{\delta_V}{\beta_V} - \frac{\delta_B}{\beta_D}) & 0 \end{bmatrix}.$$

From this, it is easily seen that the interior equilibrium, when it exists, is always asymptotically stable. Moreover, there are (damped) oscillations about the interior equilibrium whenever

$$\frac{\delta_B \beta_V}{4\beta_D^2} < 1 - \frac{\delta_V}{\beta_V} - \frac{\delta_B}{\beta_D}.$$

We were unable to find analytical expressions for the interior equilibrium $(\widehat{V}_3, \widehat{B}_3, \widehat{D}_3, \widehat{E}_3)$ in Model 1, but we can make several observations. First, since the first equation is the same in Models 1 and 2, we see that the equilibrium values of B satisfy the same equation relative to the equilibrium uninfected fraction:

$$\widehat{B} = \frac{\beta_V \widehat{E} - \delta_V}{\beta_D}, \quad \widetilde{B} = \frac{\beta_V \widetilde{E} - \delta_V}{\beta_D}.$$

Setting $\dot{E} = 0$ in each model yields equilibrium relations

$$\widehat{E} = \frac{\delta_V \widehat{V} + \delta_D \widehat{D} + \delta_B \widehat{B}}{\beta_V \widehat{V} + \beta_D \widehat{B}}, \quad \widetilde{E} = \frac{\delta_V \widetilde{V} + \delta_B \widetilde{B}}{\beta_V \widetilde{V}}.$$

While these are not the same, they have the same interpretation (and one that is common in metapopulation models, where one deals with ‘occupied’ and ‘unoccupied’ patches): the equilibrium rate at which uninfected cells are created through the death of infected cells ($\delta_V \widehat{V} + \delta_D \widehat{D} + \delta_B \widehat{B}$ in Model 1; $\delta_V \widetilde{V} + \delta_B \widetilde{B}$ in Model 2) is equal to the rate at which uninfected cells are lost through infection ($\beta_V \widehat{V} \widehat{E} + \beta_D \widehat{B} \widehat{E}$ in Model 1; $\beta_V \widetilde{V} \widetilde{E}$ in Model 2).

Numerical results of Models 1 and 2

To comprehend model behavior in ways that cannot be understood from the analyses, we provide numerical analyses. These are intended only to get the barest sense of the two models, as our main interest is in the model that includes immunity, developed in a following section.

We first compare Models 1 and 2, which differ in whether DIPs are allowed to exist with or without co-infection by virus. DIPs cannot reproduce without co-infection in both models, but allowing them to persist in an idle state prior to co-infection (Model 1) could have an effect. Fig. 1 displays short-term dynamics for the two models, side-by-side, for two sets of parameter values. The clear effect of allowing DIPs to persist in the absence of co-infection is to further suppress levels of WT virus. The figure also shows the expected damped oscillations in both models. All figures show

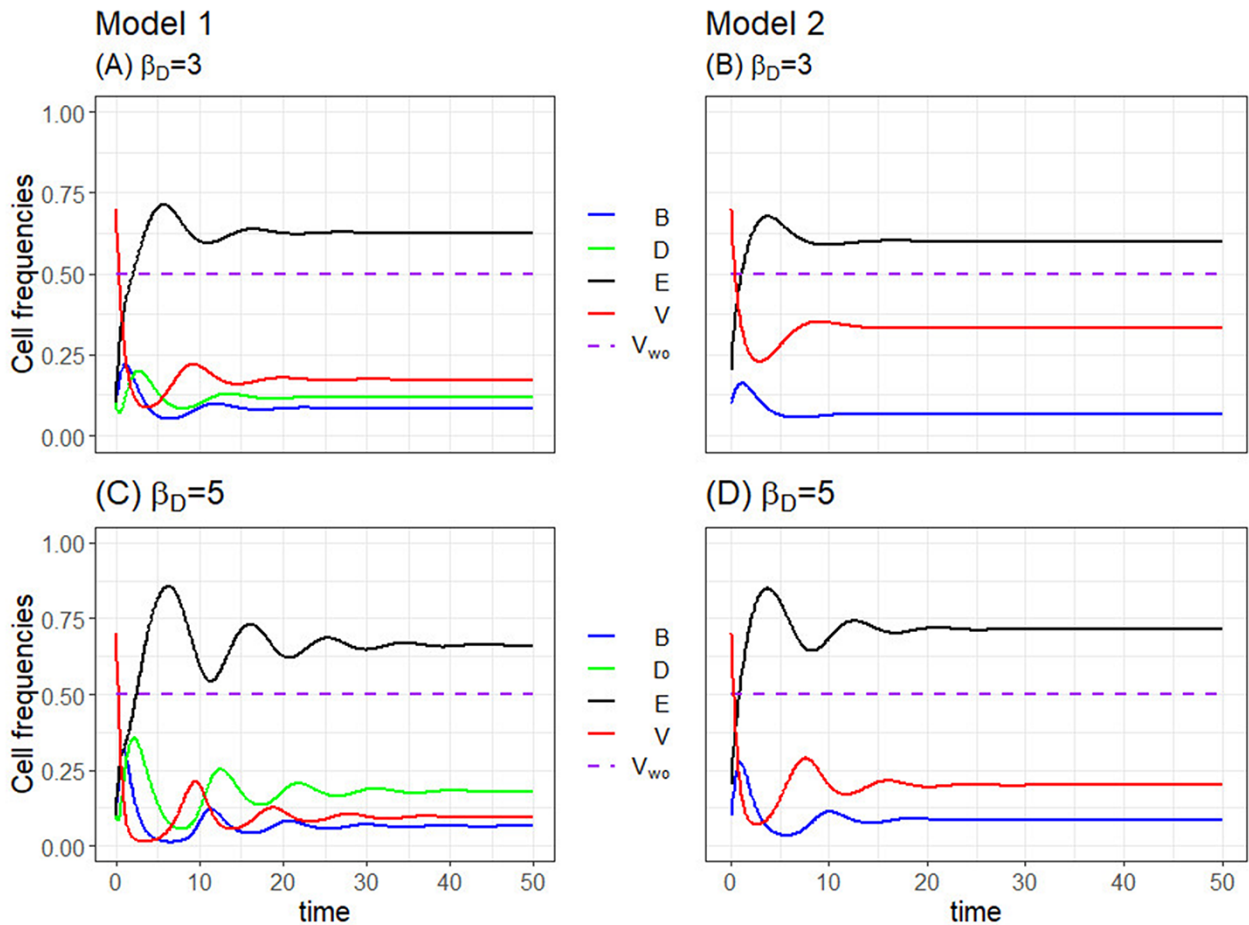


Figure 1. (Model 1 and Model 2) Comparison of the temporal dynamics for Models 1 and 2 at two different values of the DIP growth parameter. To more clearly see levels of viral suppression, the dashed line denotes the equilibrium level of virus, $V_{wo} = 1 - \frac{\delta_V}{\beta_V}$, in the corresponding simple model without any DIPs. For each value of β_D , Model 1 results in more viral suppression than Model 2 due to the ability of DIP-only infected cells to remain viable for a time. An increase in the value of β_D (as seen from top to bottom) produces more oscillations and more viral suppression. The initial values are for Model 1 are $V(0) = 0.7$, $D(0) = 0.1$, $B(0) = 0.1$, $E(0) = 0.1$. The initial values are for Model 2 are $V(0) = 0.7$, $B(0) = 0.1$, $E(0) = 0.2$. The fixed parameters are $\beta_V = 2$, $\delta_V = 1$, $\delta_D = 1$, $\delta_B = 1$.

the equilibrium frequency of virus in the absence of DIPs (dashed line), and suppression is evident. However, DIPs do not extinguish virus, as could be inferred from the equilibrium condition Equation (3).

Fig. 2 displays dynamics for Model 1, this time starting with a lower initial V , and illustrates the effect of different death rates of DIP-only cells (δ_D). The case of $\delta_D = \infty$ is equivalent to Model 2. There is a clear effect that increasing the longevity of DIP-only cells increases suppression of the virus. Also, if we compare Panel (C) in Fig. 2 with Panel (A) in Fig. 1, both of which have the same parameter values but different initial V , we see that there is a stronger DIP response (and there are larger oscillations) when DIPs are introduced at higher levels of virus. This is consistent with previous empirical work (Thompson, Rempala and Yin, 2009) showing that DIP production is higher in the presence of larger virus densities.

The trials shown in the first two figures are limited to comparisons of few parameter values. Fig. 3 shows a contour map of the suppressive effect of DIPs across a span of DIP ‘fecundity’ (β_D) and death (δ_D) values. Here, the results show how much the equilibrium frequency of virus frequency is depressed by DIPs (necessarily never exceeding one)—comparing the equilibrium

viral frequency in the absence of DIPs to that in the presence of DIPs. The strongest effect is of fecundity (β_D), but it is especially noteworthy that the magnitude of effect is substantial across β_D in the interval [1, 5].

These results merely support what already seems intuitive. The longer that ‘free’ DIPs can persist, the larger their impact on viral suppression. (The extreme is Model 2, in which they do not persist at all.) DIPs indeed suppress viral densities, but they do not extinguish the virus (both of which were well established in a previous work). We next add immunity to the model, which can clear the virus—with or without DIPs.

Adding immunity

Adding immunity to the system changes the kinds of outcomes possible. One major change is that, since we are considering acute infections, the virus will be cleared whether or not DIPs are present. This has two consequences to the analyses: (1) the impact of DIPs can be quantified in ways not possible above (e.g. there is a time to clearance and a finite cumulative viral density) and (2) the timing of DIP introduction (e.g. as a

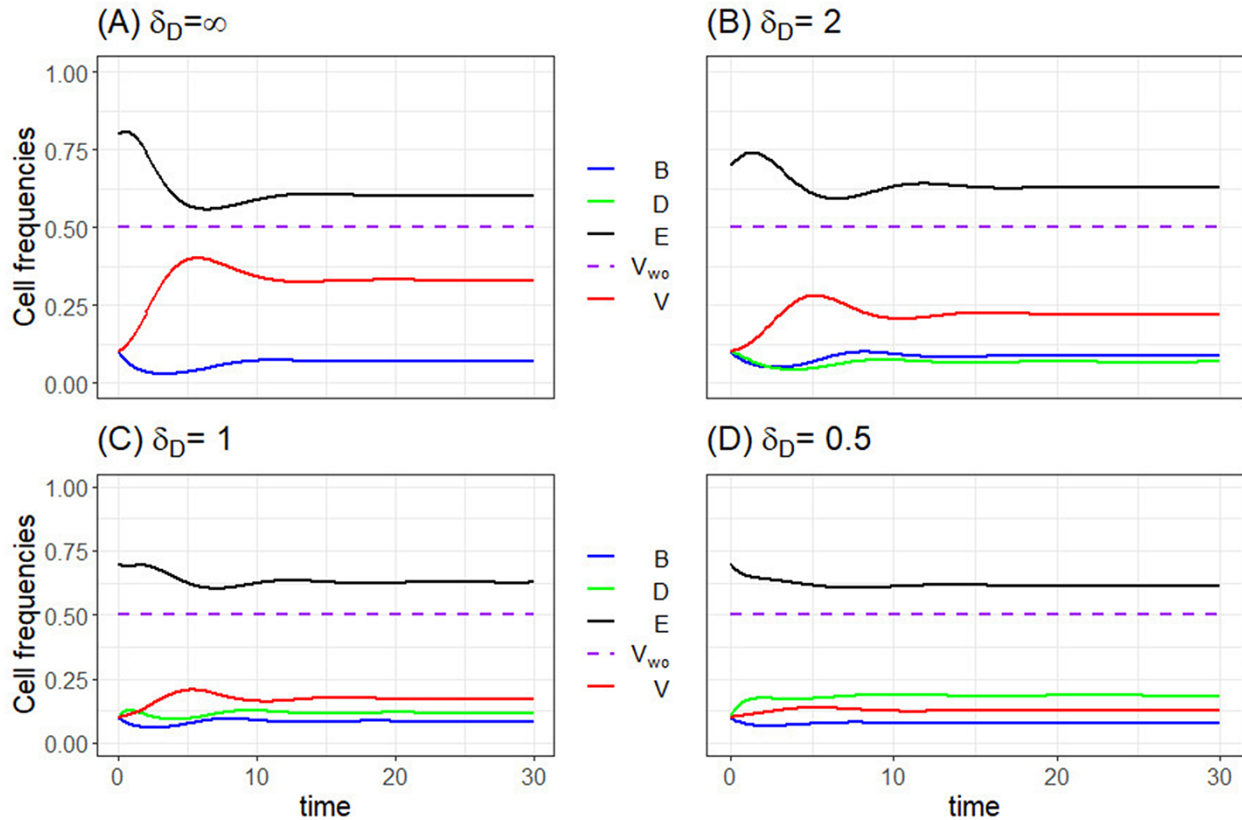


Figure 2. (Model 1) Temporal dynamics for different values of δ_D in Model 1. The dashed line represents the equilibrium value of V in the corresponding simple model without DIPS, here $1 - \frac{\delta_V}{\beta_V} = 1/2$. The case $\delta_D = \infty$ corresponds to Model 2, where we have analytical expressions for equilibrium quantities. In particular, the equilibrium value of V when $\delta_D = \infty$ is $\frac{\delta_B}{\beta_D} = 1/3$, and we see that the equilibrium amount of virus suppression compared to when no DIPS are present in the model is $1 - \frac{\delta_V}{\beta_V} - \frac{\delta_B}{\beta_D} = 1/2 - 1/3 \approx .167$. Passing to the full Model 1 and lowering δ_D results in further suppression of V . This additional suppression of V corresponds roughly to the level of D . The initial values are $V(0) = 0.1$, $D(0) = 0.1$, $B(0) = 0.1$, $E(0) = 0.7$. The fixed parameters are $\beta_V = 2$, $\delta_V = 1$, $\beta_D = 3$, $\delta_B = 1$.

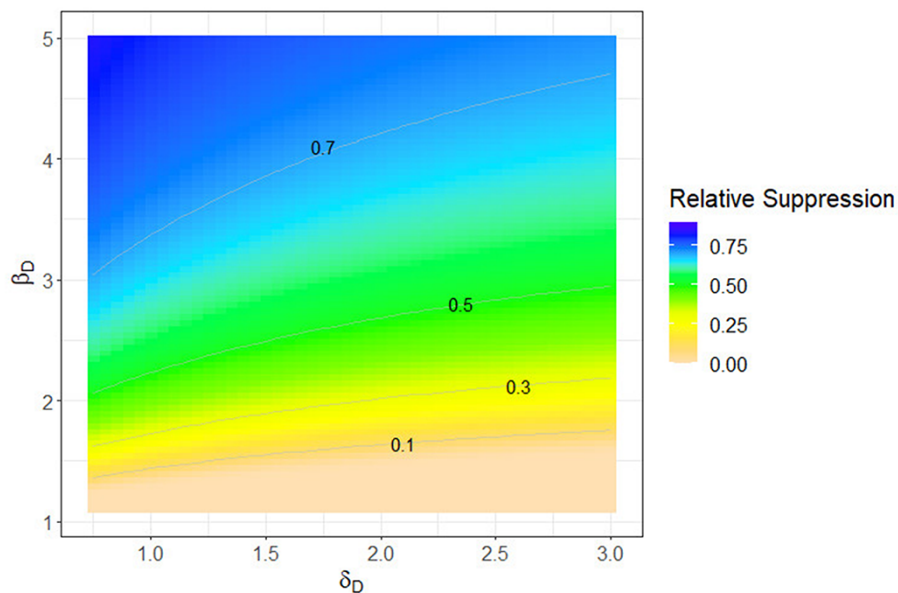


Figure 3. (Model 1) Relative suppression of WT virus by DIPS at equilibrium. We plot the relative difference, $(V_{wo} - V_w)/V_{wo}$, between the equilibrium virus levels without DIPS ($V_{wo} = 1 - \frac{\delta_V}{\beta_V}$) and with DIPS (V_w), in the absence of any immune response, as a function of the parameters δ_D and β_D . For example, the level of WT virus can be reduced by 70 per cent by introducing DIPS with $\beta_D = 3$, $\delta_D = 0.75$. The fixed parameters are $\beta_V = 2$, $\delta_V = 1$, $\delta_B = 1$.

Table 2. Description of state variables and parameters unique to Model 3.

Notation	Description	Values
I	Innate immunity level	$[0,1]$
A	Adaptive immunity level	$[0,\infty)$
k_{ij}	Killing rate of cell types $j \in \{V, B, D\}$ by immune component $i \in \{I, A\}$	$0, 1$
s_{ij}	Activation rate of innate immunity by cell types $j \in \{V, B, D\}$	$0, 0.1$
s_A	Activation rate of adaptive immunity in response to the level of innate immunity	5
d_I	Decay rate of innate immunity	0.5

therapeutic) now matters because the virus will be cleared even in the absence of DIPs.

Another major effect of adding immunity is that it introduces a possible conflict with DIPs. Both DIPs and immunity act to suppress the WT virus, but both are also boosted by the presence of virus. Thus, DIPs work in concert with immunity to suppress the WT virus, but any suppression of virus by either DIP or immunity feeds back to interfere with the continued expansion of both inhibitors. Moreover, both arms of the immune system may suppress DIPs, and both might even be stimulated by DIPs. Indeed, innate immunity has been found to be stimulated by DIPs in some systems (Rabinowitz and Huprikar, 1979; Yount, 2006; Yount et al., 2008; Killip, 2013). These interactions could therefore operate in various ways, in the extreme, with immunity suppressing DIPs and rendering them ineffective or with immunity against virus being enhanced by DIPs and resulting in a more efficient clearance of the infection that lowers both the maximum and cumulative viral load.

Model 3 extends Model 1 by adding simple characterizations of innate immunity, I , and of adaptive immunity, A . Thus, we continue to include free DIPs. Innate immunity responds quickly to virus and is self-limiting, whereas adaptive immunity responds more slowly but can expand indefinitely and persists indefinitely. Our formulation of both immunities adopts the characterization from a prior model (Antia, Ahmed and Bull, 2021). For convenience, Model 3 is displayed so that new equations and terms that distinguish it from Model 1 are separated by spaces. Model variables and parameters unique to Model 3 are presented in Table 2.

Model 3: DIPs + Immunity

$$\begin{aligned}
\dot{V} &= \beta_V V E - \beta_D B V - \delta_V V - k_{IV} I V - k_{AV} A V \\
\dot{B} &= \beta_D B V + \beta_V V D - \delta_B B - k_{IB} I B - k_{AB} A B \\
\dot{D} &= \beta_D B E - \beta_V V D - \delta_D D - k_{ID} I D - k_{AD} A D \\
\dot{E} &= -\dot{B} - \dot{V} - \dot{D} \\
\dot{I} &= (1 - I)(s_{IV} V + s_{IB} B + s_{ID} D) - d_I I \\
\dot{A} &= s_A A I
\end{aligned} \tag{6}$$

Our analyses of Model 3 focus on a few questions:

1. How does immunity change the broad outcomes of infection in the presence of DIPs?
2. How does the timing of DIP delivery affect their impact?

3. How does the effect of immunity against DIPs affect the course of the virus?

These questions are explored numerically. Although many of our figures display temporal dynamics, we also consider maximum viral density ($\max V$) and cumulative viral density over the lifetime of infection (area under the V curve or AUC). Our analyses are limited to initial conditions in which virus and immunity are both at low levels, as that initial state should represent the onset of an infection.

Comparing the broad effects of DIPs and immunity

Fig. 4 shows the separate and combined effects of DIPs and immunity for a common set of initial conditions, with DIPs administered at the start of the infection. Effects of each, together and separately, are evident. Adaptive immunity is somewhat slow to arise and, in the absence of DIPs, allows the virus to attain high levels but causes viral extinction. In contrast, DIPs have an early effect but do not extinguish the virus. When applying the $\max V$ criterion, the impression from this limited set of trials is that DIPs have the bigger effect in suppressing high viral loads. This figure is limited to DIPs being administered early in the infection, and the full spectrum of immunity is assumed—both adaptive and innate immunity are activated by and suppress both DIPs and virus.

Effect of DIP parameters on viral suppression

Contour plots of maximum viral load and cumulative viral load provide a sense of the importance of DIP parameter values in suppressing the virus when immunity is also present (Fig. 5). For DIPs to be highly effective, they especially need high fecundity, although a low death rate of free DIPs also helps. These patterns hold for both measures of viral suppression.

DIP timing matters

One challenge in applying DIPs therapeutically is in knowing when to apply them. If they decay rapidly in the absence of an infection, then advance treatment will not be practical. Instead, DIPs would often be administered after an infection was apparent, which could possibly be mid-term or late. It is thus important to know whether DIPs can be effective when delayed. As there are many variables to consider (timing and which components of immunity recognize and inhibit DIPs), we provide several figures of results.

Fig. 6 plots two summary statistics (AUC and $\max V$) across a wide range of DIP introduction times. There are minima for both statistics that approximately coincide at just under $\text{time}=4$. Timing clearly matters, but perhaps it is surprising that the earliest possible introduction is not the best—DIPs start decaying if the virus is still rare. For further insight, Fig. 7 shows the dynamics for four different introduction times. Trials vary in the extent of a ‘shoulder’ (i.e., viral rebound) in viral density. We interpret this shoulder as reflecting the separation of the effect of DIPs (which suppresses but does not clear) and immunity (which clears but whose effect is delayed). The $\text{time}=5$ panel shows the most pronounced shoulder, and the ascent of adaptive immunity is somewhat delayed compared to the other panels, an effect we interpret as due to the early suppression by DIPs.

To develop a sense of how outcomes depend on parameter values, we offer two other figures. Fig. 8 summarizes the effects of two DIP introduction times ($t=0$ and $t=4.6$) when varying δ_D and β_D . It is easily seen that the magnitude of effect of DIP timing depends on parameter values, although the relative effect

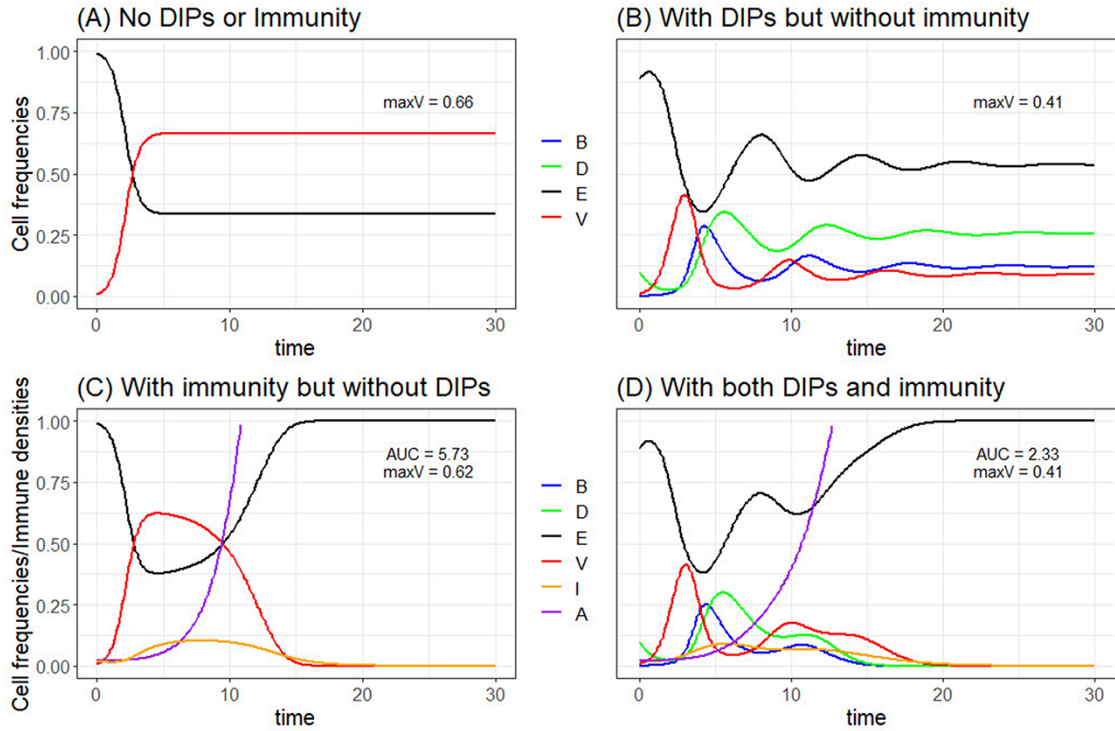


Figure 4. (Model 1 and Model 3) Comparing the effects of DIPs and/or immunity against neither for the initial thirty time units. (A) Dynamics in the absence of DIPs and immunity. As noted in prior sections, virus (V) attains a steady state and is not eliminated. (B) Dynamics with DIPs and without immunity. In contrast to the absence of DIPs (A), oscillations occur and virus is greatly suppressed over the long term. Again, virus persists indefinitely. (C) Dynamics with immunity but without DIPs. The curves demonstrate the response of V and innate and adaptive immunity when V is introduced at a low concentration. Virus attains a high density early (as in (A)) but is eventually extinguished. (D) Dynamics with both DIPs and immunity. The effect of DIPs is evident in the early suppression of virus (compared to (C)), whereas the effect of immunity is evident in eventually extinguishing the virus. Initial values are $V(0) = 0.01, B(0) = 0$, and (A) $D(0) = 0.0, E(0) = 0.99, I(0) = 0.0, A(0) = 0.0$; (B) $D(0) = 0.1, E(0) = 0.89, I(0) = 0.0, A(0) = 0.0$; (C) $D(0) = 0.0, E(0) = 0.99, I(0) = 0.02, A(0) = 0.02$; (D) $D(0) = 0.1, E(0) = 0.89, I(0) = 0.02, A(0) = 0.02$. The fixed parameters are $\beta_V = 3, \delta_V = 1, \beta_D = 5, \delta_D = 1, \delta_B = 1, k_{IV} = 1, k_{AV} = 1, k_{IB} = 1, k_{AB} = 1, k_{ID} = 1, k_{AD} = 1, s_{IV} = 0.1, s_{IB} = 0.1, s_{ID} = 0.1, d_I = 0.5, s_A = 5$.

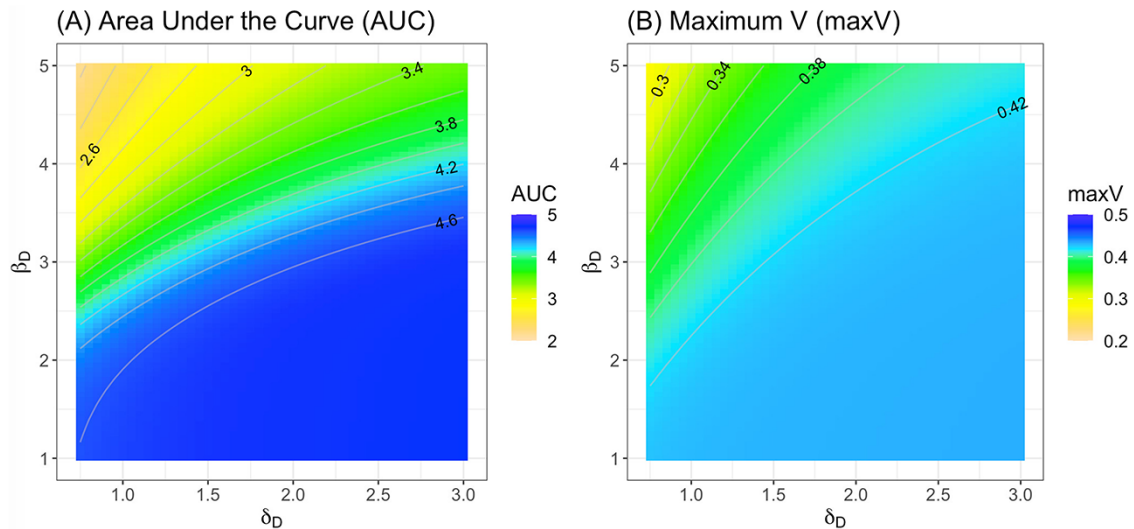


Figure 5. (Model 3) Contour plots for AUC and maximum V (maxV) in the presence of DIPs and immunity. DIPs were introduced at time=0. (A) Area under the $V(t)$ curve as a function of the parameters β_D and δ_D . (B) The maximum viral load as a function of the fecundity and death parameters β_D and δ_D . Both plots show a strong effect of fecundity interacting with the DIP death rate. The initial values for both plots are $V(0) = 0.01, D(0) = 0.1, B(0) = 0, E(0) = 0.89, I(0) = 0.02, A(0) = 0.02$, and the fixed parameters are $\beta_V = 2, \delta_V = 1, \delta_B = 1, k_{IV} = k_{AV} = k_{IB} = k_{AB} = k_{ID} = k_{AD} = 1, s_{IV} = s_{IB} = s_{ID} = 0.1, d_I = 0.5, s_A = 5$. The step size between the parameter values is 0.05 for both AUC and maxV.

(red versus blue) is nearly always the same. Fig. 9 likewise captures the temporal abundance of virus under two times of DIP introduction and for a large span of DIP fecundity (β_D). For large

values of β_D and DIPs introduced near the time of maximal efficacy, the shoulder of viral abundance becomes a second peak. This second peak is a remnant of the oscillations observed in

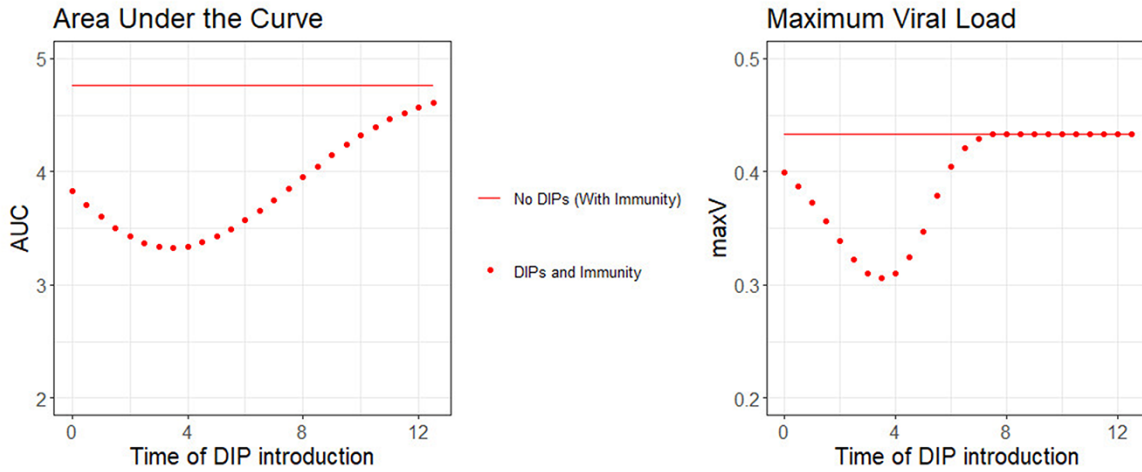


Figure 6. (Model 3) AUC and maxV with different timing of DIP introduction. DIPs are effective across a broad range of introduction times, but there is a clear optimum for both statistics. The statistic maxV becomes insensitive to DIP introduction after time=8, whereas AUC has some effect out to time=12. Initial values: No DIPs (with immunity): $V(0) = 0.01, D(0) = 0, B(0) = 0, E(0) = 0.99, I(0) = 0.02, A(0) = 0.02$; Both DIPs and Immunity: $V(0) = 0.01, D(0) = 0, B(0) = 0, E(0) = 0.99, I(0) = 0.02, A(0) = 0.02$, with an abrupt change at the indicated time t , increasing D from 0 to 0.1 and reducing E by 0.1. The fixed parameters are $\beta_V = 2, \delta_V = 1, \beta_D = 3, \delta_D = 1, \delta_B = 1, k_{IV} = 1, k_{AV} = 1, k_{IB} = 1, k_{AB} = 1, k_{ID} = 1, k_{AD} = 1, s_{IV} = 0.1, s_{IB} = 0.1, s_{ID} = 0.1, d_I = 0.5, s_A = 5$.

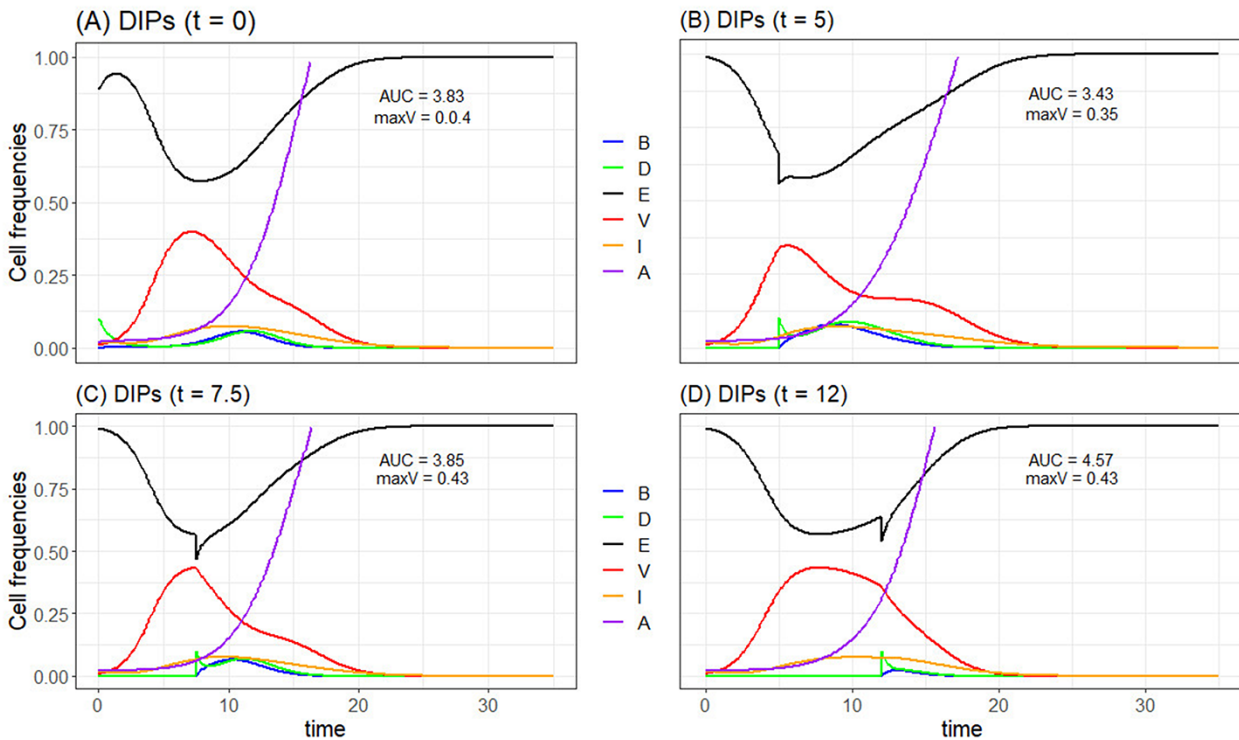


Figure 7. (Model 3) Viral and immune dynamics with DIP introduction at different times. Fig. 6 gave summary statistics of the effect of different DIP introduction times; this figure shows the full dynamics at four different introduction times. The main observation evident here is a strong shoulder of viral density when DIPs are introduced at the near-optimal time for suppression. By comparison across panels, this shoulder stems from DIPs suppressing but not clearing the infection, but there is a slightly delayed adaptive immune response. Initial values: in Panel (A), $V(0) = 0.01, D(0) = 0.1, B(0) = 0, E(0) = 0.89, I(0) = 0.02, A(0) = 0.02$; in Panels (B–D), $V(0) = 0.01, D(0) = 0, B(0) = 0, E(0) = 0.99, I(0) = 0.02, A(0) = 0.02$, with an abrupt change at the indicated time t , increasing D from 0 to 0.1 and reducing E by 0.1. The fixed parameters are $\beta_V = 2, \delta_V = 1, \beta_D = 3, \delta_D = 1, \delta_B = 1, k_{IV} = 1, k_{AV} = 1, k_{IB} = 1, k_{AB} = 1, k_{ID} = 1, k_{AD} = 1, s_{IV} = 0.1, s_{IB} = 0.1, s_{ID} = 0.1, d_I = 0.5, s_A = 5$.

Models 1 and 2 (immunity absent) and would not occur if immunity responded faster.

Immunity can act in a myriad of ways: does it matter?

We have thus far modeled immunity as the most extreme possible: free DIPs stimulate both adaptive and innate immunity

and are killed by both. (Of course, we have not used the most extreme parameter values possible.) How much change in control of the virus will occur if DIPs are not stimulatory or killed? In Fig. 10, we compare several of these alternatives for two introduction times. When comparing cumulative (AUC) and maximal viral titers (maxV) across the different changes in immunity

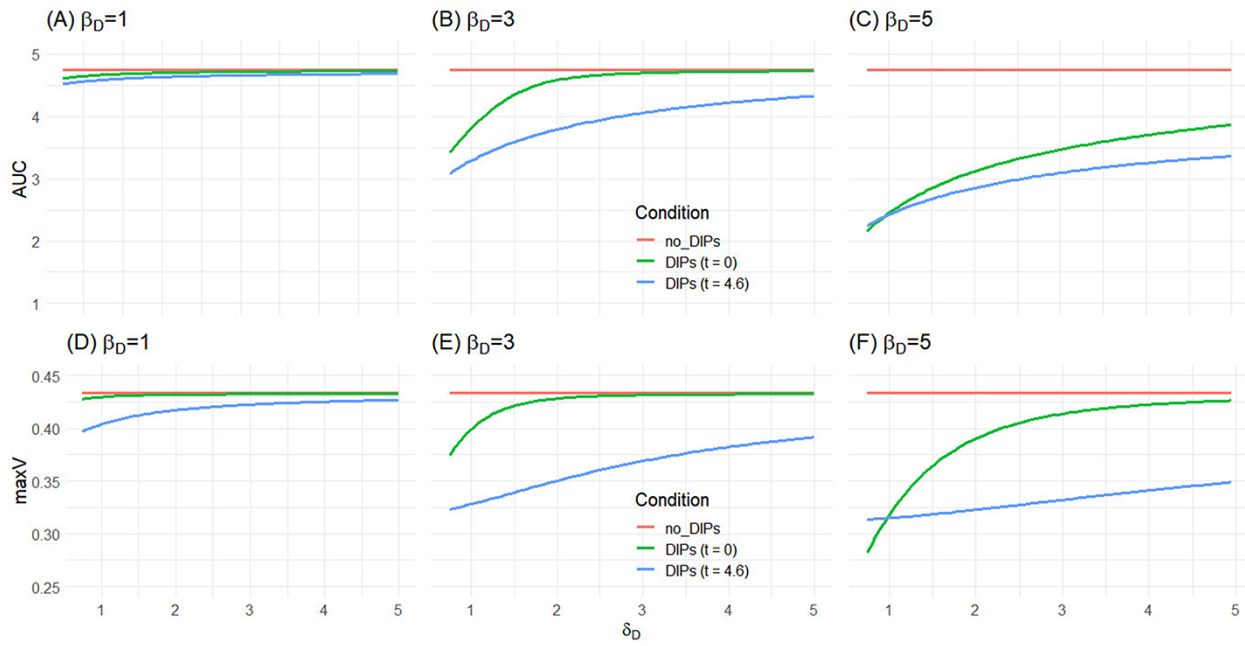


Figure 8. (Model 3) Measures of infection load caused by the virus (V) as a function of DIP parameters (β_D and δ_D) and the time of DIP introduction (early versus late). The top row plots total viral load (AUC) given by the AUC. The bottom row plots maximum viral load (maxV). For reference, the straight red lines indicate AUC and maxV in the model with immunity but no DIPs. The immune system always clears the virus. The middle (green) curves plot these quantities when DIPs are introduced at the start of the simulation, along with the virus; the lower (blue) curves correspond to waiting to introduce DIPs until the viral level has first reached 30 per cent (which occurs at $t = 4.6$). The graphs show that the introduction of DIPs lessens the severity of the infection relative to what it would be with only the immune response. Moreover, waiting to introduce DIPs until the virus has increased in frequency is more effective than introducing them at the beginning. The initial values are (red curve) no DIPs: $V(0) = 0.01, D(0) = 0, B(0) = 0, E(0) = 0.99, I(0) = 0.02, A(0) = 0.02$; (green curve) DIPs at $t = 0$: $V(0) = 0.01, D(0) = 0.1, B(0) = 0, E(0) = 0.89, I(0) = 0.02, A(0) = 0.02$; (blue curve) DIPs at $t = 4.6$: $V(0) = 0.01, D(0) = 0, B(0) = 0, E(0) = 0.99, I(0) = 0.02, A(0) = 0.02$. In case (3), DIPs are administered at the time, $t = 4.6$, when V first reaches 0.3, i.e. $V(4.6) = 0.3$; at this time, D jumps from 0 to $D(4.6) = 0.1$ and E is reduced by 0.1 to keep total cell density equal to 1. No other quantities are adjusted. The fixed parameters are $\beta_V = 2, \delta_V = 1, \delta_B = 1, k_{IV} = k_{AV} = k_{IB} = k_{AB} = k_{ID} = k_{AD} = 1, s_{IV} = s_{IB} = s_{ID} = 0.1, d_I = 0.5, s_A = 5$.

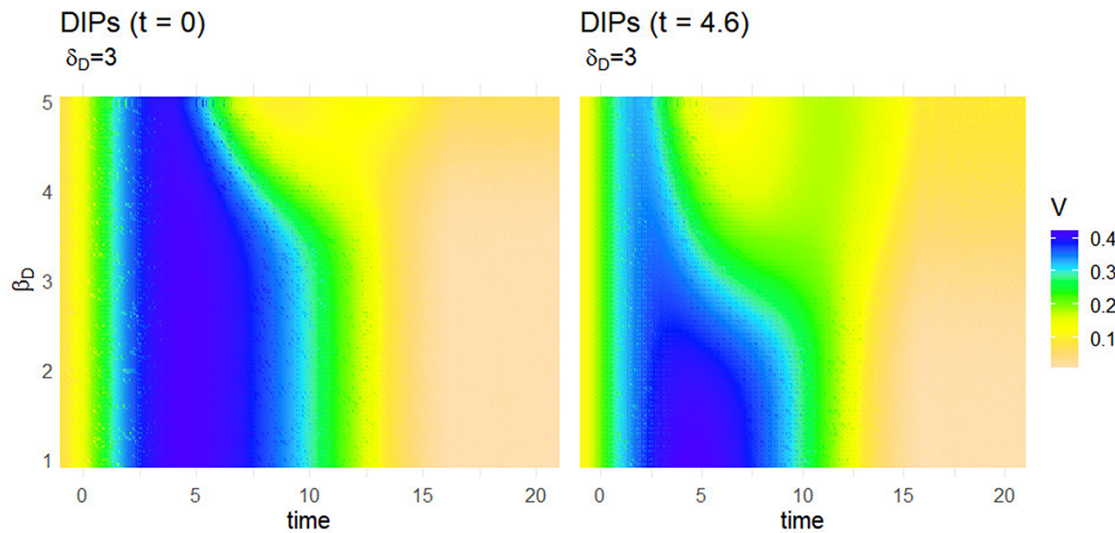


Figure 9. (Model 3) Temporal behavior of V for different values of β_D in cases where DIPs are introduced at $t = 0$ (left) and at $t = 4.6$ (right), with immunity ultimately clearing the virus. There is a compression of V that begins when β_D reaches a value of approximately three. The effect of this compression is more noticeable when DIPs are added later ($t = 4.6$, which is when the virus first reaches level 0.3) than when they are added at the beginning. One also sees a smaller second wave of V when DIPs are added at the later time, for high values of β_D . The initial values and fixed parameters are as in Fig. 8, except that we fix $\delta_D = 3$ here.

parameterization, the main effect is seen to be the timing of DIP delivery. These results clearly depend on the range of immune parameter values employed, but they at least reinforce the possible beneficial effect of DIPs and the importance of timing.

Discussion

DIPs are parasites of viruses. They cannot reproduce unless their host cell is also infected with the WT, functional virus. In essence, a DIP is a parasite whose host is a virus-infected cell—thus a

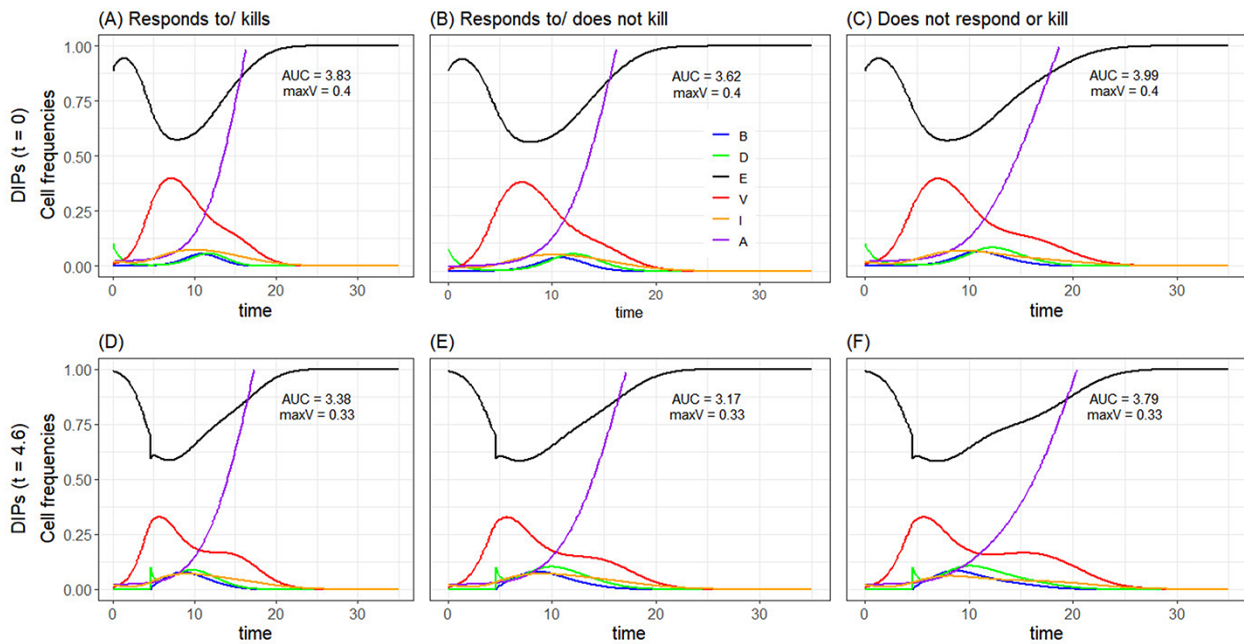


Figure 10. (Model 3) Effect of adding DIPS early (first row) or later (second row), when the immune system responds to DIPS and kills DIPS (first column), responds to DIPS but does not kill DIPS (second column), and neither responds to nor kills DIPS (third column). (A and D): the immune system responds to the presence of DIPS ($s_{IV} = s_{IB} = s_{ID} = 0.1$) and kills DIP-infected cells ($k_{IV} = k_{AV} = k_{IB} = k_{AB} = k_{ID} = k_{AD} = 1$); (B and E): the immune system responds to the presence of DIPS ($s_{IV} = s_{IB} = s_{ID} = 0.1$) but does not kill DIP-infected cells ($k_{IV} = k_{AV} = k_{IB} = k_{AB} = 1, k_{ID} = k_{AD} = 0$); (C and F): the immune system does not respond to the presence of DIPS ($s_{IV} = 0.1, s_{IB} = 0.1, s_{ID} = 0$) and does not kill DIP-infected cells ($k_{IV} = k_{AV} = k_{IB} = k_{AB} = 1, k_{ID} = k_{AD} = 0$). The initial values are $V(0) = 0.01, D(0) = 0.1, B(0) = 0, E(0) = 0.89, I(0) = 0.02, A(0) = 0.02$ in the first row, and $V(0) = 0.01, D(0) = 0, B(0) = 0, E(0) = 0.99, I(0) = 0.02, A(0) = 0.02$ in the second row, with an abrupt change at $t = 4.6$ increasing D from 0 to 0.1 and reducing E by 0.1. The fixed parameters are $\beta_V = 2, \delta_V = 1, \beta_D = 3, \delta_D = 1, \delta_I = 1, d_I = 0.5, s_A = 5$. We also ran the model in the first row, but with twice the response to DIPS: $s_{IB} = 0.2$ instead of 0.1. This resulted in AUC values of 3.67, 3.47, 3.73 and maxV values 0.4, 0.4, 0.4. (Graphs not shown.) Thus a larger innate immune response to DIPS led to improved AUC values compared to the top row, but the maxV values did not improve.

parasite of a parasite. They arise, persist, and evolve in the context of many natural infections, typically derived as genomic degenerates from the WT viral genome, and each kind of DIP is often specific to the virus it parasitizes (Horiuchi, 1983; DePolo and Holland, 1986; a; DePolo, Giachetti and Holland, 1987; Barrett and Dimmock, 1986; Marriott and Dimmock, 2010). Recently, however, the possibility of engineering DIPS has been demonstrated (Meng, 2017; Yao et al., 2021). DIPS have long been entertained as possible antiviral defenses. In addition to the obvious therapeutic benefit of suppressing the WT virus, they are commonly devoid of protein-coding genes so should—to a first approximation—have little potential for harm to any host they infect.

The practicality of DIP therapy depends on many factors, and the intuition of even the most basic properties is difficult. Theoretical explorations of DIPS are few and largely confined to DIP-virus interactions either under mass action or with spatial structure. Our main contribution here is to add an immune response to the dynamics, whereby the immune system alone can both control and eliminate the infection. The addition of DIPS thus faces several challenges, including whether DIPS are added early enough to augment the clearance as well as whether DIPS might actually interfere with the immune response.

Our study used the numerical solution of differential equation models to consider how DIPS influence an acute infection in the presence of immunity; baseline behavior was the effect of DIPS in the absence of immunity—the setting for most previous theoretical studies of DIP dynamics, and one necessary to understand the basic suppressive effect of DIPS. The main effect of immunity

is to limit the time in which DIPS can have an effect. The general message here is the intuitive one that DIPS can augment the immune response and be effective at suppressing both the maximal viral load and the cumulative load. However, the timing of DIP administration is critical, which is not a result that can be inferred from models lacking immunity. It is also noteworthy, although not surprising, that there were no phase transitions leading to qualitative changes in outcomes that could complicate the successful application of DIPS as a therapy.

Our study did not address one potential problem that is likely to confront many DIP therapies: a possible mismatch between DIP and virus and evolution of that interaction. Experimental *in vitro* evolution studies have shown that DIPS and their viral hosts co-evolve rapidly (Horiuchi, 1983; DePolo, Giachetti and Holland, 1987). For some systems, however, a robustness of certain DIPS to WT escape has been observed (Meng, 2017; Dimmock et al., 2008). For a DIP to be maximally effective, it must be well-matched to the virus being treated, but the virus being treated may quickly evolve to minimize the inhibition (whether within a single host or between hosts). The very preparation of the therapeutic DIP population needs to be tailored to its ‘host’ virus. Engineering platforms for DIP preparation may enable the preparation of relatively pure DIP populations, but it may instead be desirable to produce mixtures of DIPS that anticipate and block viral escape. This problem offers interesting challenges for research. It is especially interesting, if not surprising, that an influenza DIP appears to be robust against escape by the WT virus (Easton et al., 2011; Meng, 2017).

Data availability

The R code used to generate the data in each of the figures is publicly available on GitHub (<https://github.com/banditakarki/DIPs-project-Figures>).

References

- Akpinar, F. B., Inankur and J., Yin (2016) 'Spatial-temporal patterns of viral amplification and interference initiated by a single infected cell', *Journal of Virology*, 90: 16 7552–7566.
- Alnaji, F. G. and C. B., Brooke (2020) 'Influenza virus DI particles: Defective interfering or delightfully interesting?' *PLOS Pathogens*, 16: 5 e1008436.
- Antia, R., H., Ahmed and J. J., Bull (2021) 'Directed attenuation to enhance vaccine immunity', *PLoS Computational Biology*, 17: 2 e1008602.
- Bangham, C. M. and T. B. L., Kirkwood (1990) 'Defective interfering particles: Effects in modulating virus growth and persistence', *Virology*, 179: 2 821–826.
- Barrett, A. D. and N. J., Dimmock (1986) 'Defective interfering viruses and infections of animals', *Current Topics in Microbiology and Immunology*, 128: 55–84.
- DePolo, N. J., C., Giachetti and J. J., Holland (1987) 'Continuing coevolution of virus and defective interfering particles and of viral genome sequences during undiluted passages: virus mutants exhibiting nearly complete resistance to formerly dominant defective interfering particles', *Journal of Virology*, 61: 2 454–464.
- DePolo, N. J. and J. J., Holland (1986) 'The intracellular half-lives of nonreplicating nucleocapsids of DI particles of wild type and mutant strains of vesicular stomatitis virus', *Virology*, 151: 2 371–378.
- ____ 'Very rapid generation/amplification of defective interfering particles by vesicular stomatitis virus variants isolated from persistent infection', *The Journal of General Virology*, 67: Pt 6) 1195–1198.
- Dimmock, N. J. and A. J., Easton (2014) 'Defective interfering influenza virus RNAs: time to reevaluate their clinical potential as broad-spectrum antivirals?' *Journal of Virology*, 88: 10 5217–5227.
- Dimmock, N. J. et al. (2008) 'Influenza virus protecting RNA: an effective prophylactic and therapeutic antiviral', *American Society for Microbiology*, 82: 17 8570–8578.
- Easton, A. J. et al. (2011) 'A novel broad-spectrum treatment for respiratory virus infections: influenza-based defective interfering virus provides protection against pneumovirus infection in vivo', *Vaccine*, 29: 15 2777–2784.
- Frank, S. A. (2000) 'Within-host spatial dynamics of viruses and defective interfering particles', *Journal of Theoretical Biology*, 206: 2 279–290.
- Horiuchi, K. (1983) 'Co-evolution of a filamentous bacteriophage and its defective interfering particles', *Journal of Molecular Biology*, 169: 2 389–407.
- Killip, M. J. et al. (2013) 'Deep sequencing analysis of defective genomes of parainfluenza virus 5 and their role in interferon induction', *Journal of Virology*, 87: 9 4798–4807.
- Kirkwood, T. B. and C. R., Bangham (1994) 'Cycles, chaos, and evolution in virus cultures: a model of defective interfering particles', *Proceedings of the National Academy of Sciences*, 91: 18 8685–8689.
- Marriott, A. C. and N. J., Dimmock (2010) 'Defective interfering viruses and their potential as antiviral agents', *Reviews in Medical Virology*, 20: 51–62.
- Meng, B. et al. (2017) 'Unexpected complexity in the interference activity of a cloned influenza defective interfering RNA', *Virology Journal*, 14: 1 138.
- Rabinowitz, S. G. and J., Huprikar (1979) 'The influence of defective-interfering particles of the PR-8 strain of influenza a virus on the pathogenesis of pulmonary infection in mice', *Journal of Infectious Diseases*, 140: 3 305–315.
- Thompson, K. A. S., G. A., Rempala and J., Yin (2009) 'Multiple-hit inhibition of infection by defective interfering particles', *Journal of General Virology*, 90: 4 888–899.
- Thompson, K. A. S. and J., Yin (2010) 'Population dynamics of an RNA virus and its defective interfering particles in passage cultures', *Virology Journal*, 7: 1 1–10.
- Vignuzzi, M. and C. B., López (2019) 'Defective viral genomes are key drivers of the virus-host interaction', *Nature Microbiology*, 4: 7 1075–1087.
- Yao, S. et al. (2021) 'A synthetic defective interfering SARS-CoV-2', *PeerJ*, 9: e11686.
- Yount, J. S. et al. (2008) 'MDA5 participates in the detection of paramyxovirus infection and is essential for the early activation of dendritic cells in response to Sendai virus defective interfering particles', *The Journal of Immunology*, 180: 7 4910–4918.
- Yount, J. S. et al. (2006) 'A novel role for viral-defective interfering particles in enhancing dendritic cell maturation', *The Journal of Immunology*, 177: 7 4503–4513.